Simulation of Manufacturing Process of Ceramic Matrix Composites

Dr. Sergei.P. Yushanov, Dr. Jeffrey.S. Crompton and Dr. Kyle.C. Koppenhoefer*, ACES of Columbus.
*Corresponding author: 750E Cross Pointe Rd, Columbus, OH 43230. kyle@acescolumbus.com

Abstract: Improved performance of aero-engines achieved by increasing the operating temperature requires the development of new manufacturing technologies for ceramic matrix composites (CMCs). Manufacturing of CMCs has been simulated using COMSOL Multiphysics. Specialized simulation technologies have been developed to describe the infiltration of molten material into a ceramic perform. The physical phenomena considered in the analysis includes: unsaturated flow, capillary fluid flow, reaction between the fluid and matrix, volumetric changes associated with the fluid-solid reaction, temperature changes associated with the fluid-solid reaction and residual stress development. The resulting simulation allows a more accurate analysis of the process and identification of the significance of the interdependent physical phenomena in the manufacturing process. Application of simulation tools of this type will provide designers with the opportunity to reduce cycle time, increase part yield, and optimize the process window for CMC manufacturing.

Keywords: CMCs, unsaturated flow, residual stress, aero-engine.

1. Introduction

Increasing the temperature at which jet aircraft engines operate can provide significant improvements in thrust and fuel efficiency and at the same time provide reduced emissions. However, current engines operate within 50 degrees of the melting point of conventional materials, thus new materials capable of operating at higher temperatures for prolonged times must be developed and manufactured. Ceramics and ceramic matrix composites (CMCs) can operate at temperatures in excess of 2000°F but are difficult to fabricate into the complex shapes required for jet engine use and consequently novel manufacturing processes must be developed and processing conditions optimized for routine production of complex components.

To support the development of innovative manufacturing processes required for the production of CMCs, specialized multiphysics simulation tools have been developed to simulate the infiltration of molten material into a ceramic perform. Results of these analyses will allow designers to understand the significance of the multiple physical phenomena inherent in reactive melt infiltration processing to be identified.

2. Physical Phenomena

Ceramic matrix composites (CMCs) for advanced aero engine application can be produced by the infiltration of molten material into a ceramic perform. For CMCs of interest for advanced aero engine applications the molten material and perform are selected to provide a reaction between the molten metal and the preform as the liquid front advances. COMSOL Multiphysics has been used to develop specialized multiphysics simulation technologies that describe this process of reactive melt infiltration (RMI). The range of physical phenomena associated with the RMI process is large and includes the following critical mechanisms:

- Unsaturated flow of fluid into a ceramic matrix
- Capillary fluid flow
- Chemical reaction between the fluid and the ceramic matrix
- Volumetric changes associated with the fluid-solid reaction
- Temperature changes associated with the fluid-solid reaction
- Residual stress development
- Distortion of components

3. Analysis Methodology

Fluid flow described using Richard's and Darcy's equations have been coupled with partial

differential equations describing the chemical reaction between the fluid and the ceramic matrix. Simultaneously, heat transfer in a porous media associated with both the liquid and solid phase, and thermal and dilational strains associated with the anisotropy of the mechanical properties of the composite material are solved. The resulting simulation is a simultaneous solution that incorporates the relevant, multiple physical phenomena that describe the manufacturing of CMCs.

Unsaturated flow through a porous media has been simulated using Richard's equation:

$$(C + S_e S)\frac{\partial P}{\partial t} + \nabla \bullet \left(-\frac{\kappa_s}{\eta}\kappa_r \nabla (P + \rho_f g D) \right) = 0 .$$

Within this solution, the initial and boundary conditions are defined as:

$$P\big|_{t=0} = -P_c$$
$$P\big|_{inlet} = +P_{in}$$

where

P_c: capillary pressure
P_{inlet}: inlet pressure

In addition to Richard's equation, this work considered the effects of using a formulation based on Darcy's law. In this formulation the fluid velocity in the unsaturated media is

$$\mathbf{u}_{esvr} = -\frac{\kappa_s}{\eta}\kappa_r \nabla (P + \rho_f g D) .$$

where:

κ_s : intrinsic permeability at saturation

κ_r : relative permeability

η : fluid viscosity

ρ_f : fluid density,

g: gravitational acceleration

S_e: effective saturation

$S = \rho_f g (\chi_f + \chi_s)$ storage coeff.

χ_f : compressibility of fluid

χ_S : compressibility of solid preform

C: specific moisture capacity

D: direction of gravity action

The effective saturation, relative permeability, and moisture capacity are functions of pressure:

$$Se = Se(P),\ \kappa_r = \kappa_r(P),\ S = S(P, \theta_s).$$

The reaction kinetics of the SiC where calculated using a general reaction kinetics equation with constants for the Si+C reaction:

.

$$\frac{\partial \theta_{SiC}}{\partial t} + \mathbf{u} \bullet \nabla \theta_{SiC} = r(\theta_f - \theta_{SiC})^{\beta}$$

Where:

θ_f : volume fraction of fluid

θ_{SiC} :volume fraction of SiC

$r = r_0 e^{-\frac{E}{RT}}$: reaction rate

r_0 : reaction rate at reference T

β : reaction constant

Velocity $\mathbf{u}$ of moving fluid is defined by:

$$\mathbf{u} = \begin{cases} \mathbf{u}_{esvr} & (filling\ \ stage\ :\ t \le t_{fill}) \\ 0 & (cooling\ \ stage\ :\ t > t_{fill}) \end{cases}$$

The volume fraction of Si is obtained as:

$$\theta_{Si} = \theta_f - \theta_{SiC}$$

Subject to the following boundary conditions

$$\theta_{SiC}\big|_{t=0} = 0$$
$$\nabla \theta_{SiC}\big|_{\Gamma} = 0 .$$

The above mass balance assumes that reaction proceeds to full completion, and all Si transforms into SiC. To account for the effect of reaction termination, mass balance can be modified as:

$$\frac{\partial \theta_{SiC}}{\partial t} + \mathbf{u} \bullet \nabla \theta_{SiC} = r(\alpha_f \theta_f - \theta_{SiC})^{\beta}$$

Where

α_f is the degree of conversion of Si

Heat transfer from the exothermic reaction was calculated using available energy balance approaches:

$$C_{eq}\frac{\partial T}{\partial t} + \nabla \bullet (-K_{eq}\nabla T) + C_{PL}\mathbf{u} \bullet \nabla T = Q_H .$$

To account for the liquid and solid phases within the heat transfer problem, volume average

equivalent thermal conductivity K_{eq} and heat capacity C_{eq} of porous media are given by:

$$K_{eq} = \frac{\theta_L k_L + \theta_S k_S}{\theta_L + \theta_S}$$

$$C_{eq} = \frac{\rho_L C_{PL} \theta_L + \rho_S C_{PS} \theta_S}{\theta_L + \theta_S}$$

where subscripts "L" refers to liquid phase and subscripts "S" refers to solid perform. The residual stress developed was calculated using integrated solid mechanics to solve the equilibrium equation:

$$\nabla \bullet \boldsymbol{\sigma} = 0$$

with the following constitutive relation:

$$\boldsymbol{\sigma} = \mathbf{C} : \boldsymbol{\varepsilon}_{el}$$

where:

$\mathbf{C}$: elastic tensor

$\boldsymbol{\varepsilon}_{el}$: elastic strain

4. Results and Discussion

Limited experimental data is available (1, 2) to allow extensive validation of the analytical routines developed here. Validation exercises have been performed for a limited number of cases in which appropriate experimental data exists. The predicted effect of changing pore size on infiltration is compared with experimental data in Figure 1.

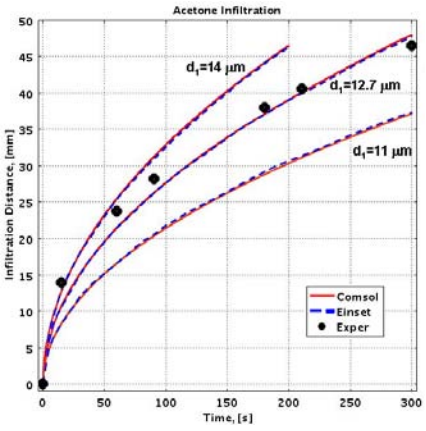

Figure 1. Comparison of analytical and experimental results for the infiltration of acetone into performs with various pore sizes.

The infiltration profile for a range of nonreactive fluids is shown in Figure 2.

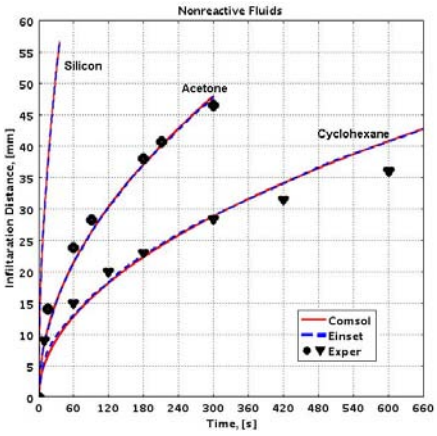

Figure 2. Calculated and experimental infiltration profiles for cyclohexane, acetone and nonreactive silicon.

In contrast the predicted influence of reaction between the infiltrating fluid and the matrix is shown in Figure 3 and is compared to experimental conditions under which reaction occurs between the fluid and matrix.

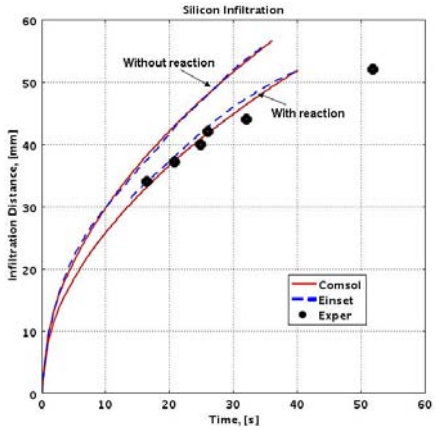

Figure 3. Calculated and experimental infiltration profiles for flow of silicon into ceramic perform showing the influence of reaction between the fluid and perform.

In all case excellent agreement is obtained between the experimental data and the results of the analytical routines developed here.

Typical results of analyses to explore the effects of different parameters that affect the processing of CMCs can be provided by the analytical routines developed during this work. Examples of the predicted distributions of unsaturated flow, energy balance, and reaction kinetics during the filling stage, t = 1s are shown in

Figure 4. Analyses were performed on a quarter symmetric model; the vertical line represents the boundary between the 90° and 0° layers; the 90° layer appears on the right side of the model.

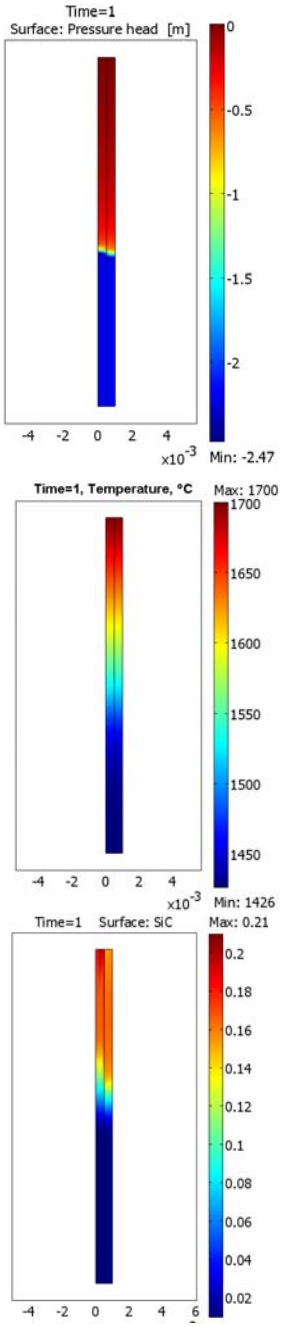

Figure 4. Distribution of (a) Pressure head, (b) Temperature, and (c) SiC volume fraction during the filling state at t = 1 s.

Figure 5 shows the liquid volume fraction as a function of time at y=0 and indicates that both the 90° and 0° layers are filled with fluid at t = 4s. The contour plot in Figure 5 shows the spatial variation in liquid volume fraction at t = 3s.

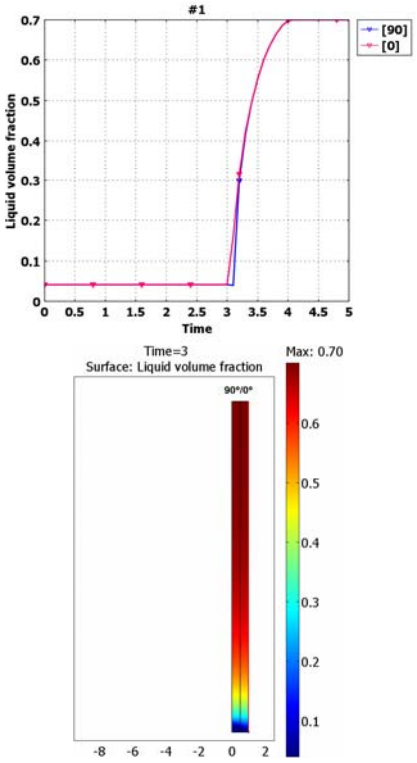

Figure 5. (a) Liquid volume fraction in the 90°/0° layers at the y=0 symmetry plane, and (b) contour plot of the liquid volume fraction at t=3s

The filling times of the two layers are equal; however the fluid velocity behind the unsaturated flow differs for the 90° and 0° layers. The spatial distribution of velocity in the direction of flow at t=1s is given in Figure 3. Figure 6(a) shows the flow front at approximately y=0.0095m where local flow from the 0° layer to the 90° layer maintains the overall balance.

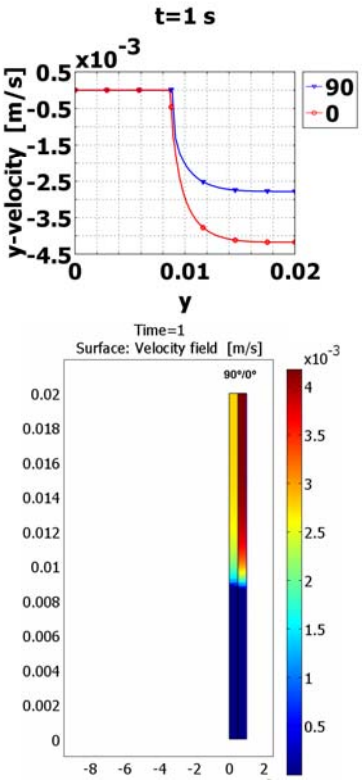

Figure 6. Distribution of the velocity in the fill direction for both layers at t=1s.

Figure 7 clearly indicates the fluid transfer mechanism with silicon flowing from the 0° to the 90° layer.

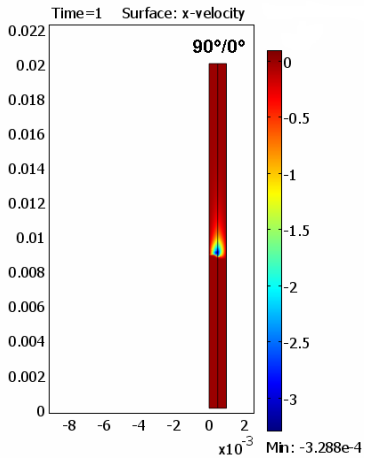

Figure 7. Transverse velocity component at t=1s.

Figure 8 shows the distribution of the liquid volume fraction and the velocity. In Figure 5(a), the unsaturated flow front propagates in the negative y direction. Figure 8(b) shows that the velocity of the unsaturated flow interface decreases as filling proceeds. Velocity is highest at the initial stage of filling and decreases as the region becomes more saturated. This decrease results from Darcy's law and that flow is driven by capillary pressure. Initially, when the region is fully unsaturated, the capillary pressure is high. As fluid flows in, saturation levels increase, capillary pressure decreases, and the velocity of the unsaturated flow interface decreases.

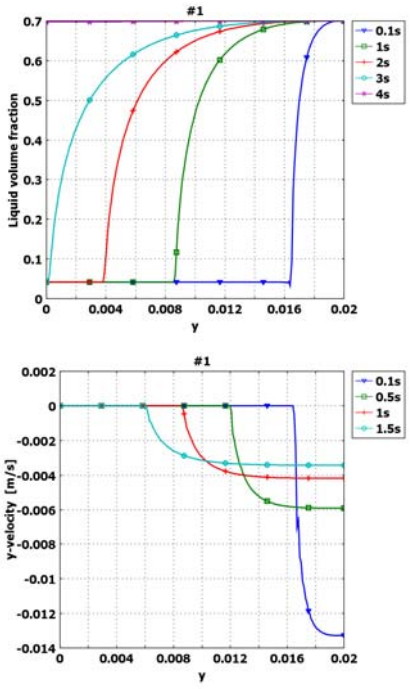

Figure 8. Evolution of the unsaturated flow interface at $x = 0$ (a) liquid volume fraction and (b) vertical velocity

Figure 9 shows the distribution of SiC and Si species along $x = 0$ at discreet time instances. The convection of the moving fluid and the reaction rate define the distribution of both species. The sum of the volume fractions of Si and SiC equals the total volume fraction of fluid.

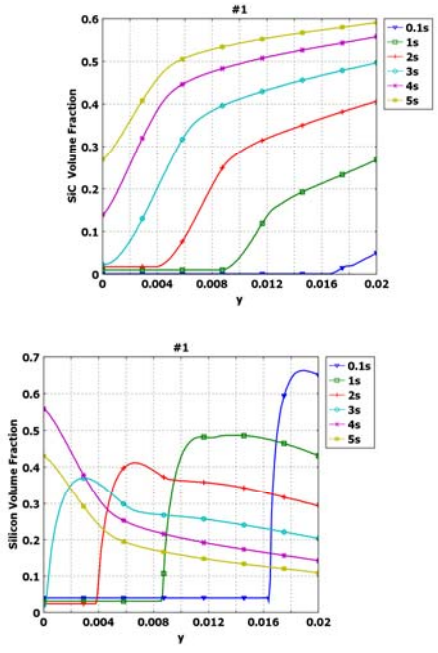

Figure 9. Distribution of (a) SiC and (b) Si volume fractions along $x = 0$ at discreet times.

The temperature distribution along the length of the preform is given in Figure 10. Initially, temperature is preheat temperature(1425˚C) and the temperature of the incoming fluid is T_{inlet}=1700˚C. As the fluid flows, the temperature of the preform increases and the temperature gradient decreases. The analyses include the heat released due to the continuous exothermic reaction of the C and Si species.

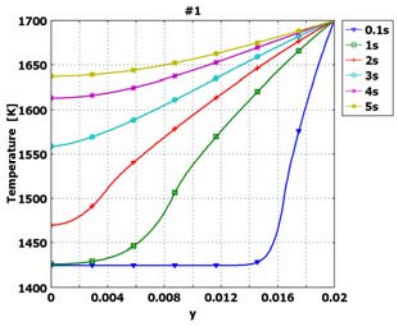

Figure 10. Temperature distribution during and after the filling of the preform.

5. Conclusions

This work demonstrates the numerical representation of the different physical phenomena associated with a CMC manufacturing process. The numerical results are stable over a wide range of model parameters. The accuracy of the numerical results can be increased significantly by refining the physical parameters in the system. Porosity and permeability ratio have a nearly linear effect on filling time. However, the effect of capillary pressure is strongly nonlinear. A better understanding of the reaction kinetics could provide additional insight into the heating of the preform.

6. References

1. Einset, E. “Analysis of reactive melt infiltration in the processing of ceramics and ceramic composites”, *Chemical Eng. Sci.*, Volume 53, No 5, pp1027-1038 (1998)

2. Einset, E. “Capilliary infiltration rates into porous media with applications to silcomp processing”, *J. Am. Ceram. Soc.*, Volume 79, No 2, pp333-338 (1996)